Available online at http://www.ijasrd.org/in

International Journal of Advanced Scientific Research & Development

Vol. 02, Iss. 03, Ver. II, Jul – Sep' 2015, pp. 149 – 158

e-ISSN: 2395-6089
p-ISSN: 2394-8906

INVESTIGATIONS ON THE STRUCTURAL, OPTICAL, MECHANICAL AND MICROSTRUCTURAL PROPERTIES OF L–ARGININE DOPED SAP CRYSTALS – A POTENTIAL MATERIAL FOR NLO APPLICATIONS

Dr. M. Iyanar[1]

[1] Assistant Professor of Physics, National College, Trichy.

Dr. J. Thomas Joseph Prakash[2]

[2] Assistant Professor of Physics, Government Arts College, Tiruchirappalli.

S. Ekadevasena[3]

S. Shek Dhavud[3]

J. Martin Sam Gnanaraj[3]

[3] Final Year Students, Department of Physics, National College, Trichy.

ARTICLE INFO

Article History:

Received: 24 Sep 2015;
Received in revised form:
28 Sep 2015;
Accepted: 28 Sep 2015;
Published online: 30 Sep 2015.

Key words:

NLO Material,
SEM,
Semiorganic,
SHG

ABSTRACT

The growth of L-Arginine doped SAP crystals were attained by Slow Evaporation Solution Growth Technique. Structural, Spectral, Optical and Morphological properties were investigated by various characterizations. SEM analysis reveals the uniform distribution of particles on the surface. Optical analysis shows the transparency of the grown crystal in the visible region. Hence the title material can be used for NLO device applications.

INTRODUCTION

Phthalic acid derivatives are potential compounds for NLO and electro-optic processes. The semiorganic hydrogen phthalate crystals are widely used in the applications of long-wave X-ray spectrometers. Alkali Acid Phthalate crystals are used as substrates for deposition of thin films of organic nonlinear materials[1]. Sodium Acid Phthalate single crystal is an excellent compound for SHG applications in the phthalic acid family. There are only a few reports available on the effect of amino acid on the NLO efficiency of SAP crystals. Crystalline Phthalic acid complexes have been subjected to extensive investigations by several researchers so as to study about their linear and nonlinear optical properties. In general, Phthalate complexes are being widely investigated for their

How to cite this article: Iyanar, M., Prakash, T. J. J., Ekadevasena, S., Dhavud, S. S., & Gnanaraj, M. S. J., (2015). "Investigations on the Structural, Optical, Mechanical and Microstructural Properties of L–Arginine Doped SAP Crystals – A Potential Material for NLO Applications". *International Journal of Advanced Scientific Research & Development (IJASRD), 02* (03/II), pp. 149 – 158.

promising electronic and optoelectronic applications[2-10]. The crystallographic data for many phthalic acid complexes exists in the literature are the salts of Potassium Acid Phthalate (KAP), Sodium Acid Phthalate (SAP), and Lithium Acid Phthalate (LiAP)[11-13]. All these compounds are stabilized by extensive networks of hydrogen bonds. The influence of strong and weak hydrogen bonds on the nonlinear behaviour of the crystals have already been studied earlier[14]. Phthalate samples of sodium and potassium are promising third-order NLO materials for applications in optical devices[15-17]. L-Arginine doped Sodium Acid Phthalate has been chosen for the present study because of its favorable optical properties which has been grown by slow evaporation technique at room temperature.

EXPERIMENTAL

The slow evaporation technique was employed to synthesize Pure Sodium Acid Phthalate crystal by dissolving sodium bicarbonate and phthalic acid in deionized water in an equimolar ratio. The solution was thoroughly stirred for 2 hrs using magnetic stirrer and the saturated solution of the above synthesized salt was prepared and the undoped SAP crystals were grown at room temperature. Optically transparent and good quality crystals were collected from the mother solution after 30 days which is shown in Fig. 1. The mother solution was prepared using SAP salt in deionized water and 0.2 mole% of L-Arginine was added as a dopant in the mother solution. The saturated solution was filtered and kept for evaporation at room temperature. Optically transparent crystals of L-Arginine doped SAP crystals was obtained after 30 days which is shown in Fig. 1.

Fig. 1: *As Grown L-Arginine Doped SAP Crystal*

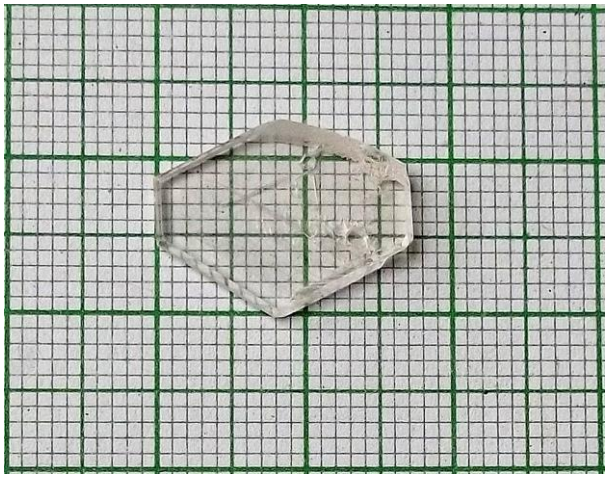

RESULTS AND DISCUSSIONS

3.1. Structural Analysis

To determine the unit cell parameters the grown pure and doped crystals were subjected to single crystal X-ray diffraction study using an ENRAFNONIUS CAD-4 diffractometer. The observed lattice parameter values of L-Arginine doped SAP crystals are shown in Table.1 which is in good agreement with the reported values[18]. The incorporation of L-Arginine into the crystal lattice of pure SAP crystal is clearly indicated by the minor deviations in the cell parameters.

Table 1: *Cell Parameters of Undoped and L-Arginine Doped SAP Crystal*

SAP Crystal[20]	L-Arginine doped SAP crystal
a= 6.75 Å	a= 6.67 Å
b= 9.31 Å	b= 9.26 Å
c= 26.60 Å	c= 26.68 Å
Volume =1662 Å^3	Volume =1679 Å^3
System= Orthorhombic	System= Orthorhombic
Space group =B2ab	Space group =B2ab

Table 2: *Comparison of Cell Values Obtained from Single Crystal and Powder XRD*

Single Crystal X-Ray diffraction	PowderX-Ray Diffraction
a= 6.67 Å	a= 6.65 Å
b= 9.26 Å	b= 9.29 Å
c= 26.68 Å	c= 26.62 Å
Volume =1679 Å^3	Volume =1645 Å^3
System= Orthorhombic	System= Orthorhombic
Space group =B2ab	Space group =B2ab

The powder X-Ray diffraction reveals the crystallinity and the phase of synthesized title material. The powder XRD pattern obtained for L-Arginine doped SAP crystals is shown in Fig.2. JEOL JDX POWDER X-RAY DIFFRACTOMETER was employed for this purpose. A set of Bragg's diffraction peaks were obtained and the miller indices are calculated using the JCPDS software (PDF. No. 321895). The cell parameters obtained from the powder x-ray diffraction analysis are calculated by the expression,

$$\lambda = 2d_{hkl} \sin\theta_{hkl} \quad \text{---------- (1)}$$

$$\frac{1}{d^2} = \left(\frac{h^2}{a^2}\right) + \left(\frac{k^2}{b^2}\right) + \left(\frac{l^2}{c^2}\right) \quad \text{---------- (2)}$$

Where,

d is the lattice spacing
hkl are the miller indices
a, b, c are the lattice parameters
λ is the wavelength of the x-ray used (CuKα = 1.5406 Å)
V is the volume of the unit cell
2θ is the diffraction angle

The obtained cell parameter values are compared with the single crystal x-ray diffraction values which presented in table-2. It is evident from the table that the title material retains its structure. The crystallite size was calculated by the Debye Scherrer's formula

$$D = 0.9\lambda/\beta\cos\theta$$

Where,

λ is the wavelength of the X-Rays used (1.540Å)
ß is the full width half maximum

θ is the Bragg's diffraction angle

The average crystallite size of the particles calculated from the powder x-ray diffraction pattern is 65 nm.

Fig. 2: *Powder XRD Pattern of L-Arginine Doped SAP Crystal*

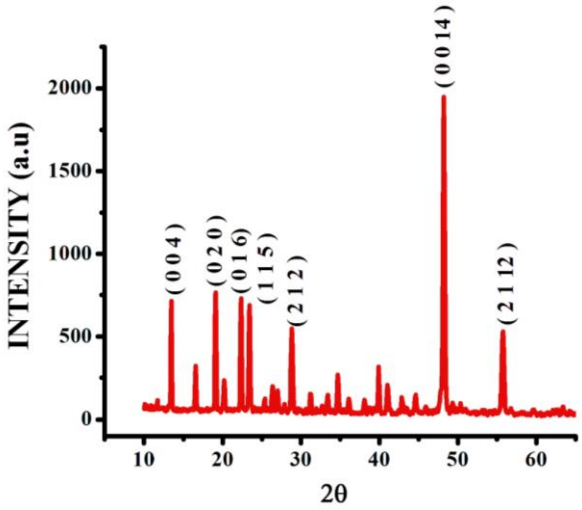

3.2. FTIR Spectral Analysis

The NH_3 asymmetric stretching vibrations are assigned to the peak at 3309 cm^{-1}. The peak at 2716 cm^{-1} confirm C-H stretching. The spectrum confirms COO^- asymmetric stretching, C-H deformation, and C-O stretching vibrations by the presence of the peaks at 1907 cm^{-1}, 1400 cm^{-1}, 1119 cm^{-1} respectively. The characteristic absorption peak at 1598 cm^{-1} is due to carboxylate ion. The double bond observed in the carboxylate ion is due to the asymmetric stretching vibration. Symmetric stretching vibration of carboxylate ion is observed at 1371 cm^{-1}. C-O stretching vibration was observed at the absorption peak at 1270 cm^{-1}. The absorption peak at 1069 cm^{-1} is attributed to C-C-O stretching vibration. C-C stretching and C-C wagging vibrations were observed at 751 cm^{-1} and 682 cm^{-1} respectively. In addition to these absorption peaks some other peaks are observed at 824 cm^{-1}, 521 cm^{-1} and 415 cm^{-1} which are attributed due to C-H out of plane bending, C=C-C out of plane ring deformation and C=C plane bending respectively.

Fig. 3: *FTIR Spectrum of L-Arginine Doped SAP Crystal*

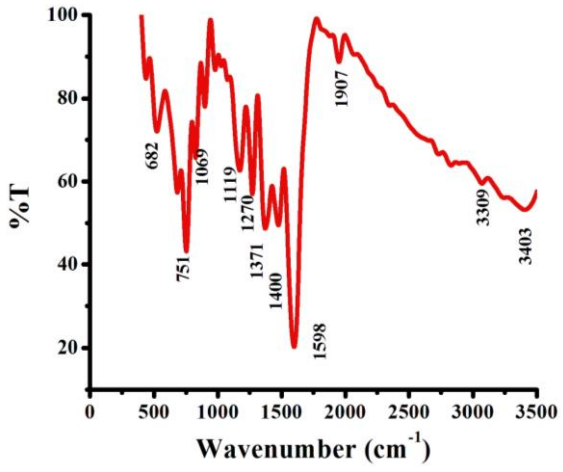

3.3 Linear Optical Analysis

UV visible NIR spectral analysis is an effective tool for identifying the optical property of the grown crystals. UV Visible The recorded UV spectrum is shown in Fig 4. From the figure it is evident that L- Arginine doped SAP crystal is transparent without any strong absorptions in the entire visible region (380-800 nm). The lower cutoff is observed around 310 nm which makes the title material a potential candidate in optoelectronic applications. Hence linear optical analysis signifies that the title material is an effective NLO material. Because of wide optical applications of NLO materials, the transmission range and transparency cut-off are very important parameters, especially for crystals used in SHG[19-21]. The crystal shows a good transmittance in the visible region. NLO crystals with high conversion efficiencies for SHG and transparent in visible and ultraviolet ranges are required for numerous device applications. The lower cut-off wavelength around 310 nm is due to the n–π transition of the carbonyl group of the carboxyl function. This transition causes its nonlinear optical responses and absorption in the near UV region. The wide range of transparency of the grown crystals is an added advantage in the field of optoelectronic applications.

Fig. 4: *UV Transmission Spectrum of L-Argininne Doped SAP Crystal*

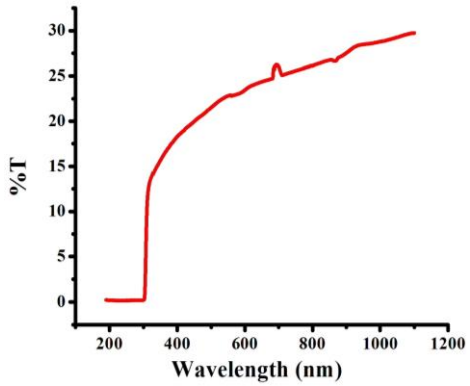

3.4 Microstructural Morphology

The microstructural morphology of the undoped and L-Arginine doped SAP crystals were analyzed by subjecting it to SEM analysis. JEOL 6360 TESCAN Scanning electron microscope was used for in this process. The SEM micrographs of L-Arginine doped SAP crystals are shown in Fig. 5(a) – 5(d). It contains almost tightly packed hexagonal-like structure with grain size around 15 – 30 nm which are uniformly distributed.

Fig. 5 (a) - 5(d): *SEM Micrographs of L-Arginine Doped SAP Crystal*

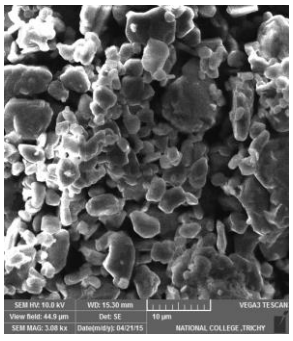

Fig. 5 (a)

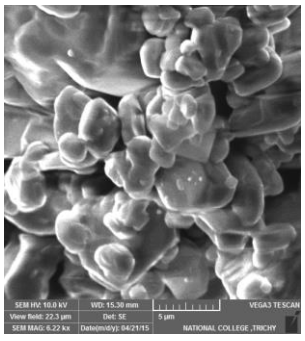

Fig. 5 (b)

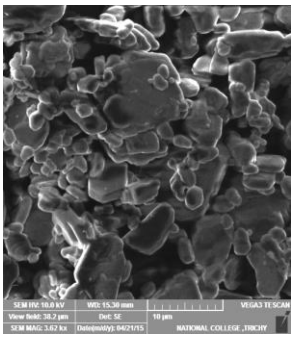

Fig. 5 (c)

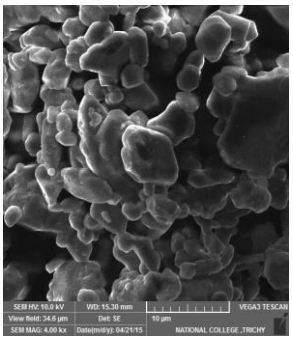

Fig 5 (d)

The magnified SEM micrograph is shown in Fig. 5(e). The substitution of L-Arginine inside the SAP lattice, induces the distortion which is responsible for grain size reduction. In addition to this, the grains are agglomerated each other with size around 50-75 nm. Tensile stress is completely relieved and the lattices are much relaxed and creates better crystallization.

Fig. 5 (e): *Magnified SEM Micrograph of L-Arginine Doped SAP Crystal*

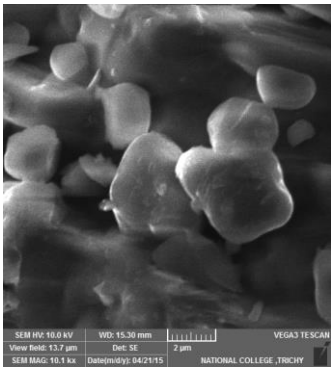

The presence of agglomerated particles suggests that the growth process starts with clusters in a colloidal state. These clusters integrate into larger particles called secondary spherical particles. This minimizes their surface energy. Then these secondary particles further collide and merge with each other forming multimers. The obtained results coincide well with the powder x-ray diffraction analysis.

3.5 Vicker's Microhardness

For post growth processes and device fabrication, the mechanical hardness of the crystal is an important parameter. Microhardness measurements were carried out using a Leitz Wetzler hardness tester fitted with a Vickers diamond pyramidal indenter and attached to a Leitz incident light microscope. The distance between any two indentations was maintained to be greater than five times that of the diagonal length in order to avoid any mutual influence of the indentations. The dwell time was 5 s for all the loads. Hardness number was calculated from the relation:

$$H_v = 1.8554p/d^2 \text{ kg mm}^{-2}$$

Where P is the applied load (in kg) and d is the diagonal length of indentation (in mm). Fig.6 clearly indicates that hardness of the grown crystals increases with increase in load and having maximum hardness number at 100 g.

Fig. 6: *Load vs Hv of L-Arginine Doped SAP*

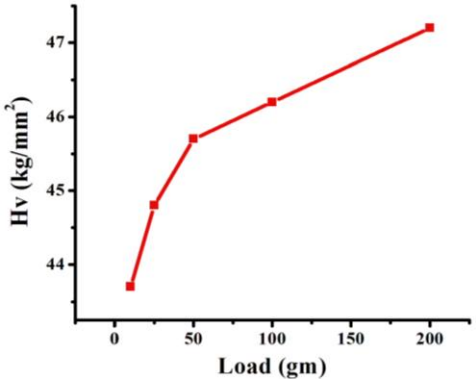

The load above 50 g develops multiple cracks on the crystal surface due to the release of internal stresses generated locally by indentation. The hardness increases with increase in load and this suggests L- Arginine doped SAP crystals are efficient candidates in NLO applications below 50 g of applied load.

3.6 Nonlinear Optical Studies

Kurtz and Perry powder technique[23] remains an extremely valuable tool for initial screening of materials for second harmonic generation (SHG).The grown crystals were subjected to the NLO study to measure the efficiency with respect to pure KDP and L-Arginine doped SAP single crystals. The SHG property of the grown crystals was tested by the Kurtz and Perry powder method. The fundamental beam of wavelength 1064 nm from a Q-switched Nd:YAG laser with a pulse energy 3 mJ/pulse, pulse width 8 ns, and repetition rate 10 Hz was used. The salt was packed in a micro capillary of uniform bore and exposed to laser radiations. The SHG conversion efficiency of L-Arginine doped SAP crystal was found to be more than that of pure KDP crystal. The optical signal generated from the sample was converted into an electrical signal and was measured using an oscilloscope. The measured outputs for pure KDP and L-Arginine doped SAP crystals were 38 mV and 52 mV respectively. This indicates that the SHG conversion efficiency of L-Arginine doped SAP crystal is 1.3 times that of pure KDP crystal. The output was confirmed by the emission of green radiation from the sample which indicates that the title material possesses NLO property. Hence L-Arginine doped SAP crystals are exploited for the generation of Green Emission radiation. Apart from this L-Arginine doped SAP crystals are best suited in the NLO and optoelectronic device fabrications.

3.7 Dielectric Studies

The dielectric study for L-Arginine doped SAP crystal was carried out using Agilent 4284-A LCR meter. The observations are made in the frequency range 100 Hz–1 MHz at room temperature. The plot of log f vs dielectric constant is depicted in Fig. 7(a). The dielectric constant decreases with increase in frequency. This effect can be attributed to the effect of charge distribution by mean carrier hopping on defects. At low frequency, the charge on the defects can be rapidly redistributed so that defects closer to the positive side of the applied field become positively charged. This leads to a screening of the field and overall reduction in the electric field. Because the capacitance is inversely proportional to the field, this reduction in the field for a given voltage results in the increased capacitance observed as the frequency is lowered. The dielectric constant of materials is due to the contribution of electronic, ionic, dipolar and space charge polarizations, which depend on the frequencies. At low frequencies, all these polarizations are active. The space charge polarization is generally active at lower frequencies and high temperatures. The variation of dielectric loss with log f is shown in Fig. 7(b). The low dielectric loss shows the crystals are of enhanced optical quality[24]. This is in good agreement with the result of optical studies and this parameter is of vital importance for various NLO devices.

Fig. 7(a): *log f vs Dielectric Constant*

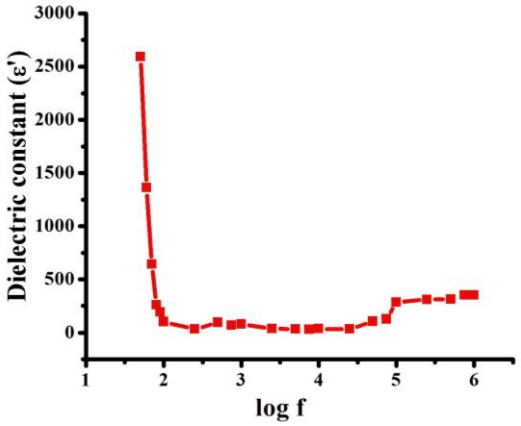

Fig. 7(b): *log f vs Dielectric Loss*

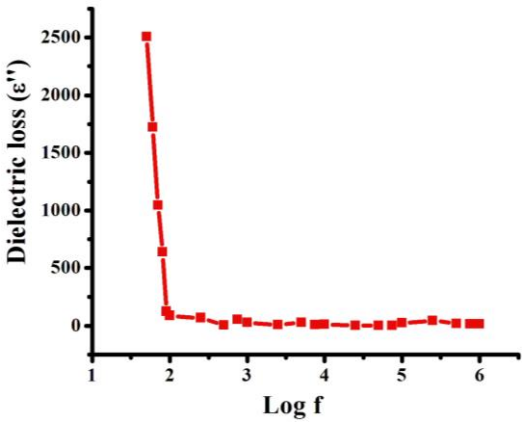

CONCLUSION

Single crystals of L-Arginine doped SAP, potential semi-organic NLO materials, has been grown from aqueous solution. The unit cell parameters of the doped crystals were determined by the single crystal X-ray diffraction study. FTIR spectra confirms the presence of functional groups qualitatively. The wide range of transparency of the grown crystals in the visible region shows the suitability of the grown materials in the field of optoelectronic applications. The hardness graph shows the hardness increases with increase in load. The SHG efficiency of the grown crystals was more than the SHG efficiency of the reference material KDP.

4.1 Acknowledgements

One of the authors Dr. M. Iyanar gratefully acknowledges the University Grants Commission, New Delhi, India for providing financial assistance for the project under Minor Research Project Scheme File Number: No.F. MRP-3207/09.

REFERENCES

[1] W. Sander Graswinckel, Fieke J. Van den Bruele, Willem J.P. Van Enchevort, Elias Vlieg, Cryst. Growth Des. 7 (2007) 243.

[2] A. Smith, "The Crystal Structures of a Series of Salts of Phthalic Acid. II. The Crystal Structure of Sodium Acid Phthalate Hemihydrate," Acta Crystallographica Section B, Vol. 51, 1975, pp. 2345-2347. doi:10.1107/S0567740875007546.

[3] H. Kuppers, "Structure of Lithium Phthalate Hemitrihydrate", Acta Crystallographica Section C, Vol. 44, No. 12, 1988, pp. 2093-2095. doi:10.1107/S0108270188008935.

[4] G. Adiwidjaja and H. Kuppers, "Lithium Hydrogen Phthalate-Methanol," Acta Crystallographica Section B, Vol. 34, 1978, pp. 2003-2005. doi:10.1107/S0567740878007190

[5] H. Kuppers, "Lithium Hydrogen Phthalate Monohydrate," Acta Crystallographica Section B, Vol. 34, 1978, pp. 3763-3765. doi:10.1107/S0567740878012121.

[6] J. S. Loring, M. Karlsson, W. R. Faweett and W. H. Casey, "Infrared Spectra of Phthalic Acid, the Hydrogen Phthalate Ion, and the Phthalate Ion in Aqueous Solution,"

Spectrochimica Acta Part A, Vol. 57, No. 8, 2001, pp. 1635-1642. doi:10.1016/S1386-1425(01)00391-2.

[7] D. S. Chemla and J. Zyss, "Nonlinear Optical Properties of Organic Molecules and Crystals," Academic Press, New York, 1987.

[8] N. Kejalakshmy and K. Srinivasan, "Growth, Optical and Electro-Optical Characterisations of Potassium Hydrogen Phthalate Crystals Doped with Fe^{3+} and Cr^{3+} Ions", Optical Materials. Vol. 27, No. 3, 2004, pp. 389-394. doi:10.1016/j.optmat.2004.09.005.

[9] J.G. Qin , D.Y. Liu, C.Y. Dai, C.T. Chen, B.C. Wu, C.L. Yang and C.M. Zhan, "Influence of the Molecular Configuration on Second-Order Nonlinear Optical Properties of Coordination Compounds," Coordination Chemistry Reviews, Vol. 188, No. 1, 1999, pp. 23-34. doi:10.1016/S0010-8545(98)00182-9.

[10] P.G. Barber and J.T. Petty, "Use of Moments of Momentum to Predict the Crystal Habit in Potassium Hydrogen Phthalate," Journal of Crystal Growth, Vol. 100, No. 1-2, 1990, pp. 185-188. doi:10.1016/0022-0248(90)90621-Q.

[11] B. Orel, D. Hadzi and F. Carassi, "Infrared and Raman Spectra of Potassium Hydrogen Phthalate," Spectrochimica Acta A: Molecular Spectroscopy, Vol. 31, No. 2, 1975, pp. 169-182. doi:10.1016/0584-8539(75)80228-5.

[12] B.N. Mavrin, M.V. Koldaeva, R.M. Zakalyukin and T.N. Turskaya, "Raman Spectra of Potassium, Rubidium, and Thallium Hydrogen Phthalates," Optika i Spektroskopiya, Vol. 100, No. 6, 2006, pp. 862-868. doi:10.1134/S0030400X06060099.

[13] N. Balamurugan, M. Lenin and P. Ramasamy, "Growth of Potassium Acid Phthalate Crystals by Sankaranarayanan-Ramasamy (SR) Method and Its Optical Characterization," Materials Letters, Vol. 61, No. 8-9, 2007, pp. 1896-1898. doi:10.1016/j.matlet.2006.07.184.

[14] G. Marudhu, S. Krishnan, G.V. Vijayaraghavan *Optik* - International Journal for Light and Electron Optics, Volume 125, Issue 10, May 2014, Pages 2417-2421.

[15] A. Senthil and P. Ramasamy, "Unidirectional Growth of Sodium Acid Phthalate Single Crystal by Sankaranarayanan-Ramasamy (SR) Method," Journal of Crystal Growth, Vol. 311, No. 23-24, 2009, pp. 4720-4724. doi:10.1016/j.jcrysgro.2009.09.014.

[16] L. Ruby Nirmala, J. Thomas Joseph Prakash. Spectrochimica Acta Part A: Molecular and Biomolecular Spectroscopy 110 (2013) 425–429 Effect of L-Valine on the growth and characterization of Sodium Acid Phthalate (SAP) single crystals.

[17] H. Kuppers, F. Takusagawa and T.F. Koetzle, "Neutron Diffraction Study of Lithium Hydrogen Phthalate Monohydrate: A Material with Two Very Short Intramolecular O...H...O Hydrogen Bonds," Journal of Chemical Physics, Vol. 82, No. 12, 1985, pp. 5636-5647. doi:10.1063/1.448550.

[18] A.K. Karnal, A. Saxena, H.L. Bhat, V.K. Wadhawan and T.P.S. Nathan, "A Novel Seed-Isolation Technique during the Processing of Solutions", Journal of Crystal Growth, Vol. 289, No. 2, 2006, pp. 617-620. doi:10.1016/j.jcrysgro.2005.11.101.

[19] W. Clegg and L. Russo, "Synthesis and Structures of Alkali Metal Complexes of Isophthalic Acid: The Interplay of Organic Supramolecular Interactions and Flexible Metal Coordination as Structure-Directing Factors," Crystal Growth & Design, Vol. 9, No. 2, 2009, pp. 1158- 1163. doi:10.1021/cg800991t.

[20] R. Bairava Ganesh, V. Kannan, K. Meera, N.P. Rajesh, P. Ramasamy, J. Cryst.Growth 282 (2005) 429.

[21] S. Krishnan, C. Justin Raj, S. Dinakaran, R. Uthrakumar, R. Robert, S. Jerome Das,J. Phys. Chem. Solids 69 (2008) 2883.

[22] Z. Sun, G. Zhang, X. Wang, Z. Gao, X. Cheng, S. Zhang, D. Xu, Cryst. Growth Des.9 (2009) 3251.

[23] S.K. Kurtz, T.T. Perry, J. Appl. Phys. 39 (1968) 3798.

[24] M. Senthil Pandian, N. Pattanaboonmee, P. Ramasamy, P. Manyum, J. Cryst. Growth 314 (2011) 207.